ME6220: HEAT EXCHANGER DESIGN

HEAT PIPES: A SURVEY & SOFTWARE DESIGN

A detailed Literature survey on heat pipes and its extensive use in modern industries, along with a MATLAB based software that can be used to design the same, with user defined inputs.

Group Members

- XXX
- Tejaswin P. (ME12B069)
- XXX
- XXX

ME6220 Project – Submitted on 04/05/ 2015

Contents

1. Abstract

Heat pipes are very flexible systems with regard to effective thermal control. They can easily be implemented as heat exchangers inside sorption and vapour-compression heat pumps, refrigerators and other types of heat transfer devices. Their heat transfer coefficient in the evaporator and condenser zones is 103–105 W/m2 K, heat pipe thermal resistance is 0.01–0.03 K/W, therefore leading to smaller area and mass of heat exchangers. This report is for partial fulfilment of the main project involving the development of a software for designing of heat pipes.

2. Introduction

The heat pipe is a device of very high thermal conductance. The idea of the heat pipe was first suggested by Gaugler in 1942. But it was only in the 1960s that it gained popularity after Grover's invention of the device.

The main regions of the standard heat pipe are shown below. In the longitudinal direction, the heat pipe is made up of an evaporator section and a condenser section, separated by an adiabatic section, if necessary. The cross section of the heat pipe, consists of the container wall, the wick structure and the vapour space.

The performance of a heat pipe is often expressed in terms of 'equivalent thermal conductivity'. A tubular heat pipe, using water as the working fluid and operated at 150ºC would have a thermal conductivity several hundred times that of copper. The power handling capability of a heat pipe can be very high - pipes using lithium as the working fluid at a temperature of 1500ºC will carry an axial flux of 1020 kW/cm2. By suitable choice of working fluid and container materials, it is possible to construct heat pipes for use at temperatures ranging from 4 K - 2300 K. For many applications, the cylindrical geometry heat pipe is suitable but other geometries can also be adopted.

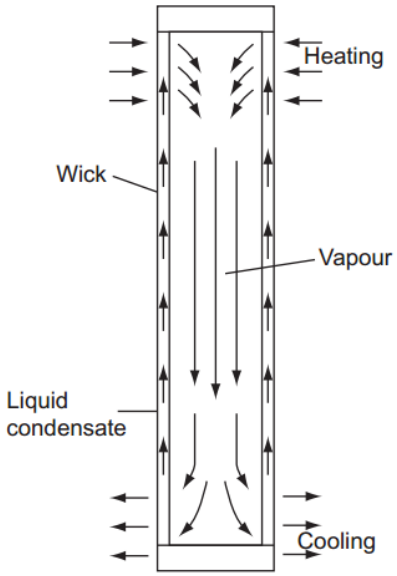

Figure 1

The superior heat transfer properties coupled with the relatively simple and flexible implementation of these devices was the primary reason for the choice of this topic and has been the motivation for development of this design software.

To understand the relevance of heat pipes to modern technology, a brief section regarding its applications has been included in this report. A basic theory regarding the working of heat pipes and the correlations used has been highlighted in the further sections. The design procedure and the logical flow of the software programme have been also been presented towards the end of this report.

3. Applications

Miniature and micro heat pipes are welcomed for electronic components cooling and space two-phase thermal control systems. Loop heat pipes, pulsating heat pipes and sorption heat pipes are the novelty for modern heat exchangers. Heat pipe air preheaters are used in thermal power plants to

preheat the secondary–primary air required for combustion of fuel in the boiler using the energy available in exhaust gases. Heat pipe solar collectors are promising developments that can be considered for domestic use.

4. Basic Theory

This section is intended to give basic and advanced users a complete introduction to the working principles behind the operation of heat pipes. There are many variants of heat pipes, but in all cases the working fluid must circulate when a temperature difference exists between the evaporator and condenser. Various analytical techniques are outlined in greater detail here, and these techniques can then be applied to the classical heat pipe and the gravity-assisted thermosyphon.

4.1. Wicked heat pipes

When constructing any heat exchanger, one tends to keep the overall thermal resistance, defined by Eq. (1), low. Even though this is also the case with the heat pipes, however, it is first necessary to ensure that the device will function correctly. The operating limits for a wicked heat pipe, as described in Ref. [1], are hence illustrated in Fig. 2.

$$R = \frac{T_{\text{hot}} - T_{\text{cold}}}{\dot{Q}} \qquad \text{.....(1)}$$

One can see that the heat pipe is restricted from various factors, namely Boiling, Sonic, Viscous, Capillary and Entrainment limit. Each of these limits may be considered in isolation as their governing equations are not coupled with each other very strongly.

In addition, for the heat pipe to operate properly, the maximum capillary pumping pressure, $\Delta P_{c\,max}$ must be greater than the total pressure drop in the pipe. This pressure drop is made up of three components:

a. The pressure drop ΔP_l required to return the liquid from the condenser to the evaporator;
b. The pressure drop ΔP_v necessary to cause the vapour to flow from the evaporator to the condenser
c. The pressure due to the gravitational head, ΔP_g (which may be zero, positive or negative, depending on the inclination)

For correct operation,

$$\Delta P_{c,\max} \geq \Delta P_{\text{l}} + \Delta P_{\text{v}} + \Delta P_{\text{g}} \qquad \text{.....(2)}$$

If this condition is not met, the wick will dry out in the evaporator region and the heat pipe will not operate. The maximum allowable heat flux for which Eq. (2) holds is referred to as the capillary limit. Methods of evaluating the four terms in Eq. (2) are discussed in detail. Typically, the capillary limit will determine the maximum heat flux over much of the operating range; however, the designer must check that a heat pipe is not required to function outside the envelope defined by the other operating limits, either at design conditions or at start-up.

During start-up and with certain high-temperature liquid metal heat pipes the vapour velocity may reach sonic values. The sonic velocity sets a limit on the heat pipe performance. At velocities approaching sonic compressibility effects must be taken into account in the calculation of the vapour pressure drop – however, we do not focus on that in this report or in the software, though necessary safeguards against the approach of this limit are taken into consideration while designing the same.

Further, the viscous or vapour pressure limit is also generally most important at start-up. At low temperature the vapour pressure of the fluid in the evaporator is very low, and, since the condenser pressure cannot be very low, the difference in vapour pressure is insufficient to overcome viscous and gravitational forces, which prevents satisfactory operation.

At high heat fluxes the vapour velocity necessarily increases, if this velocity is sufficient to entrain liquid returning to the evaporator then performance will decline. Hence the existence of an entrainment limit. The above limits relate to axial flow through the heat pipe.

The final operating limit discussed pertains to the boiling limit. The radial heat flux in the evaporator is accompanied by a temperature difference which is relatively small until a critical value of heat flux is reached - above which vapour blankets the evaporator surface, resulting in an excessive temperature difference.

It is to be noted that the position of the curves and shape of the operating envelope shown in Fig. 2 depends upon the wick material, working fluid and geometry of the heat pipe, and each of them are explained in detail in the subsequent pages.

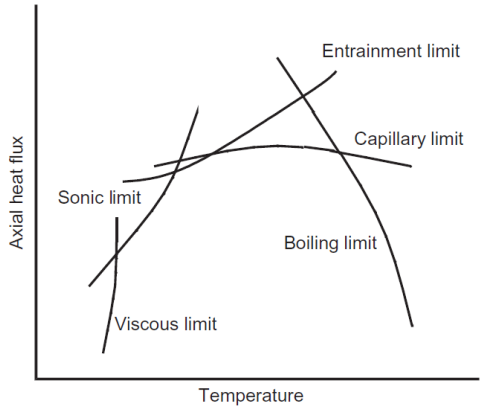

Figure 2

4.2. Gravitational Head

The pressure difference, ΔP_g, due to the hydrostatic head of liquid may be positive, negative or zero, depending on the relative positions of the condenser and evaporator. The pressure difference may be determined from:

$$\Delta P_g = \rho_l g l \sin\phi \quad \text{.....(3)}$$

Where ρ_l is the liquid density (kg/m³), g the acceleration due to gravity (9.81 m/s²), l, length of the heat pipe (m) and φ the angle between the heat pipe and the horizontal defined such that φ is positive when the condenser is lower than the evaporator. Consideration of the gravitational head is an integral part of the software designed.

4.3. Surface tension and Capillarity

4.3.1. Introduction

Molecules in a liquid attract one another. A molecule in a liquid will be attracted by the molecules surrounding it and, on average, a molecule in the bulk of the fluid will not experience any resultant force. In the case of a molecule at or near the surface of a liquid the forces of attraction will no longer balance out and the molecule will experience a resultant force inwards. Because of this effect the liquid will tend to take up a shape having minimum surface area; Due to this spontaneous tendency to contract a liquid surface behaves rather like rubber membrane under tension. In order to increase the surface area work must be done on the liquid. The energy associated with this work is known as the free surface energy, and the corresponding free surface energy/unit surface area is given the symbol, σ_l. This force/unit length is known as the surface tension. It is numerically equal to the surface energy/unit area measured in any consistent set of units.

When a liquid is in contact with a solid surface, molecules in the liquid adjacent to the solid will experience forces from the molecules of the solid in addition to the forces from other molecules in the liquid. Depending on whether these solid/liquid forces are attractive or repulsive, the liquid solid surface will curve upwards or downwards, as indicated in Fig. 2(b).

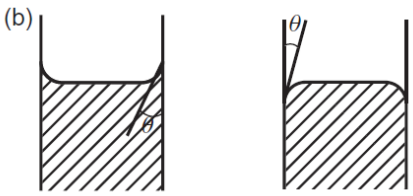

Figure 2b

Where the forces are attractive the liquid is said to 'wet' the solid. The angle of contact made by the liquid surface with the solid is known as the contact angle, θ. For wetting θ will lie between 0 and π=2 radians and for non-wetting liquids θ=π/2. The condition for wetting to occur is that the total surface energy is reduced by wetting.

$$\sigma_{sl} + \sigma_{lv} < \sigma_{sv} \qquad \text{.....(4)}$$

Where the subscripts, s, l and v refer to solid, liquid and vapour phases, respectively, as shown in Fig. 3(a). Wetting will not occur if $\sigma_{sl}+\sigma_{lv}>\sigma_{sv}$ as in Fig. 3(c) while the intermediate condition of partial wetting $\sigma_{sl}+\sigma_{lv}=\sigma_{sv}$ is illustrated in Fig. 3(b). This influences the choice of the working liquid as well as the wall and wick material. These considerations are taken in the program by introducing the values of contact angles, and having a compatibility table for the fluid and solid materials.

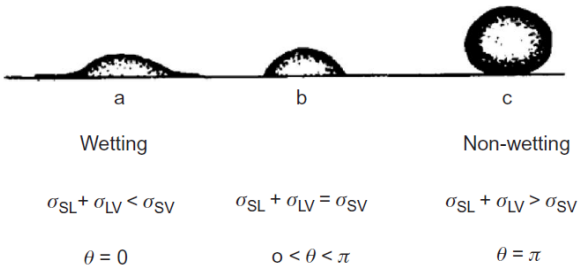

Figure 3

4.3.2. Pressure difference across a curved surface

A consequence of surface tension is that the pressure on the concave surface is greater than that on the convex surface. The governing equations are:

$$\Delta P = \frac{2\sigma_l}{R} \qquad \text{.....(5)}$$

If the surface is not spherical, but can be described by two radii of curvature, R_1 and R_2 at right angles, then it can be shown that Eq. (5) becomes:

$$\Delta P = 2\sigma_l\left(\frac{1}{R_1} + \frac{1}{R_2}\right) \qquad \text{.....(6)}$$

Due to this pressure difference, if a vertical tube, radius r, is placed in a liquid which wets the material of the tube, the liquid will rise in the tube to a height above the plane surface of the liquid as shown in Fig. 4. The governing equations for the same are:

$$(\rho_l - \rho_v)gh = \frac{2\sigma_l}{r}\cos\theta \approx \rho_l gh \qquad \text{.....(7)}$$

For the case of a non-circular tube, $\frac{1}{r} = \left(\frac{1}{R_1} + \frac{1}{R_2}\right)$

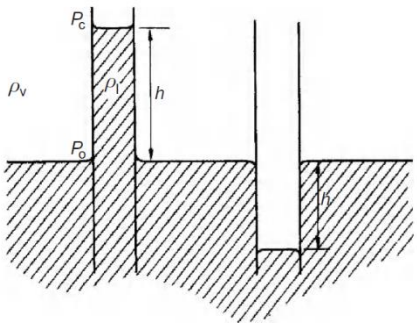

Figure 4

For non-wetting liquids $cos\theta$ is negative and the curved surface is depressed below the plane of the liquid level. In heat pipes wetting liquids are always used, the capillary lift increasing with liquid surface tension and decreasing contact angle.

4.3.3. Change in vapour pressure at a curved liquid surface

From Fig. 4 it can be seen that the vapour pressure at the concave surface is less than that at the plane liquid surface by an amount equal to the weight of a vapour column of unit area, length h.

Assuming that ρ_v is constant. Combining this with Eq. (7):

$$P_c - P_o = \frac{2\sigma_l}{r}\frac{\rho_v}{(\rho_l - \rho_v)}\cos\theta \quad \text{.....(8)}$$

this pressure difference $P_c - P_o$ is small compared to the capillary head $(2\sigma_l/r)\cos\theta$ and may normally be neglected when considering the pressures within a heat pipe. It is, however, worth noting that the difference in vapour pressure between the vapour in a bubble and the surrounding liquid is an important phenomena in boiling heat transfer.

4.3.4. Temperature dependence of surface tension

Surface tension decreases with increasing temperature, it is therefore important to take temperature effects into account if using the results of measurements at typical ambient temperatures.

Eotvos proposed a relationship which was later modified by Ramsay and Shields to give:

$$\sigma_l\left(\frac{M}{\rho_l}\right)^{2/3} = H(T_c - 6 - T) \quad \text{.....(9)}$$

where M is the molecular weight, T_c is the critical temperature (K), T the fluid temperature (K) and H is a constant, the value of which depends upon the nature of the liquid.

The Eotvos –Ramsay Shields equation does not agree with the experimentally observed behaviour of liquid metals and molten salts. Bohdanski and Schins [2] have derived an equation which applies to the alkali metals. While Fink and Leibowitz [3] recommended:

$$\sigma_l = \sigma_o\left(1 - \frac{T}{T_c}\right)^n (\mathrm{mN}/m) \quad \text{.....(10)}$$

Alternatively, the surface tension of liquid metals may be estimated from the data provided by Iida and Guthrie [4]. The value of surface tension may then be calculated using:

$$\sigma_l = \sigma_{lm} + (T - T_m)^{d\sigma/dT} \quad \text{.....(11)}$$

Values of surface tension for over 2000 pure fluids have also been tabulated by Jasper [5] and temperature corrections of the form $\sigma = a+bT$ are suggested.

4.3.5. Capillary pressure ΔP_c

Equation (5) shows that the pressure drop across a curved liquid interface is:

$$\Delta P = \frac{2\sigma_l}{R}$$

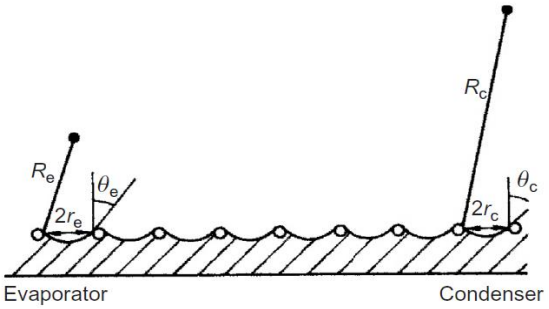

Figure 5

From Fig. 5 we can see that R cos θ = r where r is the effective radius of the wick pores and θ the contact angle. Hence the capillary head at the evaporator, $\Delta P_e'$ is:

$$\Delta P_e' = 2\sigma_l \frac{\cos\theta_e}{r_e} \quad \text{....(12)}$$

Similarly, for the condenser:

$$\Delta P_c' = 2\sigma_l \frac{\cos\theta_c}{r_c} \quad \text{....(13)}$$

and the capillary driving pressure, ΔP_c, is given by

$$\Delta P_e' - \Delta P_c'$$

It is worth noting that ΔP_c is a function only of the conditions where a meniscus exists. It does not depend on the length of the adiabatic section of the wick. This is particularly important in the design of loop heat pipes.

4.4. Pressure difference due to friction forces

In this section we will consider the pressure differences caused by frictional forces in liquids and vapours flowing in a heat pipe.

4.4.1. Laminar and Turbulent flow

If one imagines a deck of playing cards or a sheaf of papers, initially stacked to produce a rectangle, to be sheared, it can be seen that the individual cards, or lamina, slide over each other. There is no movement of material perpendicular to the shear direction.

Similarly, in laminar fluid flow there is no mixing of the fluid and the fluid can be regarded as a series of layers sliding past each other.

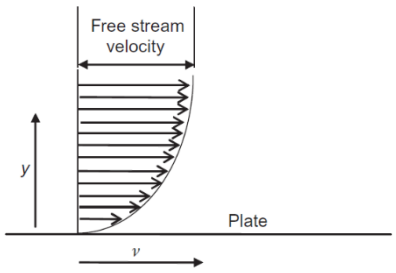

Figure 6

Consideration of a simple laminar flow allows us to define viscosity. Figure 6 illustrates the velocity profile for a laminar flow of a fluid over a flat plate.

The absolute or dynamic viscosity of a fluid, μ, is defined by:

$$\tau = \mu \frac{\mathrm{d}v}{\mathrm{d}y}$$

where τ is the shear stress. At the wall, the velocity of the fluid must be zero, and the wall shear stress is given by:

$$\tau_{\mathrm{w}} = \mu \left(\frac{\mathrm{d}v}{\mathrm{d}y} \right)_{\mathrm{w}}$$

In practice, laminar flow is observed at low speeds, in small tubes or channels, with highly viscous fluids and very close to solid walls. It is the flow normally observed when liquid flows through the wick of a heat pipe.

If the fluid layers seen in laminar flow break up and fluid mixes between the layers, then the flow is said to be turbulent. The turbulent mixing of fluid perpendicular to the flow direction leads to a more effective transfer of momentum and internal energy between the wall and the bulk of the fluid. This is illustrated in Fig. 7.

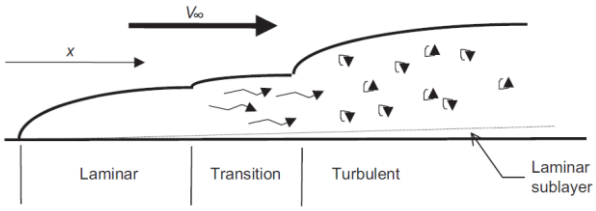

Figure 7

The heat transfer and pressure drop characteristics of laminar and turbulent flows are very different. In forced convection the magnitude of the Reynolds number, defined below, provides an indication of whether the flow is likely to be laminar or turbulent.

$$Re = \frac{\rho v^2}{\mu v / d}$$

For fully developed flow in pipes or channels the transition from laminar to turbulent flow occurs at a Reynolds number, $Re_{\mathrm{d}} = (\rho v d_{\mathrm{e}} / \mu)$ of approximately 2100. The dimension de is the channel equivalent or hydraulic diameter:

$$d_{\mathrm{e}} = \frac{4 \times \text{cross-sectional area}}{\text{wetted perimeter}}$$

4.4.2. Laminar flow: The Hagen-Poiseuille equation

The steady state laminar flow of an incompressible fluid of constant viscosity μ, through a tube of circular cross section, radius a, is described by the Hagen-Poiseuille equation.

This equation relates the velocity, v_r of the fluid at radius r, to the pressure gradient along (dp/dl) the tube.

$$v_r = \frac{a^2}{4\mu}\left[1 - \left(\frac{r}{a}\right)^2\right]\left(-\frac{dp}{dl}\right) \qquad \text{.....(14)}$$

The velocity profile is parabolic, varying from the maximum value, v_m, given by:

$$v_m = \frac{a^2}{4\mu}\left(-\frac{dp}{dl}\right) \qquad \text{.....(15)}$$

And on the axis of the tube to zero adjacent to the wall.

The average velocity, v, is given by:

$$v = \frac{a^2}{8\mu}\left(-\frac{dp}{dl}\right) \qquad \text{.....(16)}$$

or rearranging:

$$\frac{dp}{dl} = -\frac{8\mu v}{a^2} \qquad \text{.....(17)}$$

In a one-dimensional treatment the average velocity may be used throughout. The volume flowing per second, S, is:

$$S = \pi a^2 v = -\frac{\pi a^4}{8\mu}\left(-\frac{dp}{dl}\right) \qquad \text{.....(18)}$$

and if ρ is the fluid density the mass flow $\dot{m}$ is given by:

$$\dot{m} = \rho\pi a^2 v = -\rho\frac{\pi a^4}{8\mu}\left(-\frac{dp}{dl}\right) \qquad \text{.....(19)}$$

The kinetic head, or flow energy, may be compared to the energy lost due to viscous friction over the channel length l. Both may be expressed in terms of the effective pressure difference, ΔP. The kinetic energy term and the viscous term are given by,

$$\Delta P_{KE} = \frac{1}{2}\rho v^2$$
$$\Delta P_F = \frac{8\mu v}{a^2} \qquad \text{.....(20)}$$

4.4.3. Turbulent flow: The Fanning equation

The frictional pressure drop for turbulent flow is usually related to the average fluid velocity by the Fanning equation:

$$\left(-\frac{dp}{dl}\right) = \frac{4}{d}f\frac{1}{2}\rho v^2 \qquad \text{.....(21)}$$

$$\frac{P_1 - P_2}{l} = \frac{4}{d}f\frac{1}{2}\rho v^2 \qquad \text{.....(22)}$$

where f is the Fanning friction factor.

f is related to the Reynolds number in the turbulent region and a commonly used relationship is the Blasius equation:

$$f = \frac{0.0791}{Re^{0.25}}, \quad 2100 < Re < 10^5$$

The Fanning equation may be applied to laminar flow if

$$f = \frac{16}{Re}, \quad Re < 2100$$

4.5. Flow in wicks

4.5.1. Pressure difference in liquid phase

The flow regime in the liquid phase is almost always laminar. Since the liquid channels will not in general be straight nor of circular cross section and will often be interconnected, the Hagen Poiseuille equation must be modified to take account of these differences. Since mass flow will vary in both the evaporator and the condenser region, an effective length rather than the geometrical length must be used for these regions. If the mass change per unit length is constant the total mass flow will increase, or decrease, linearly along the regions, being zero at the end. We can therefore replace the lengths of the evaporator l_e and the condenser l_c by $(l_e/2)$ and $(l_c/2)$. The total effective length for fluid flow will then be l_{eff} where:

$$l_{\text{eff}} = l_{\text{a}} + \frac{l_{\text{e}} + l_{\text{c}}}{2}$$

Tortuosity within the capillary structure must be taken into account separately. There are three principal capillary geometries.

1. Wick structures consist of a porous structure made up of interconnecting pores. Gauzes, felts and sintered wicks come under this; these are frequently referred to as homogeneous wicks.

2. Open grooves.

3. Covered channels consist of an area for liquid flow closed by a finer mesh capillary structure. Grooved heat pipes with gauze covering the groove, and arterial wicks are included in this category. These wicks are sometimes described as composite wicks.

In the software, design is considered only for homogenous wicks, as design of arterial wicks require some intuition and experience, which is beyond the scope of our discussion.

4.5.2. Homogeneous wicks

If ε is the fractional void of the wick, that is the fraction of the cross section available for the fluid flow, then the total flow cross-sectional area A_f is given by:

$$A_{\text{f}} = A\varepsilon = \pi(r_{\text{w}}^2 - r_{\text{v}}^2)\varepsilon$$

where r_w and r_v are the outer and inner radius of the wick, respectively.

If r_c is the effective pore radius, then the Hagen- Poiseuille equation (Eq. (19)) may be written as:

$$\dot{m} = \frac{\pi(r_{\text{w}}^2 - r_{\text{v}}^2)\varepsilon r_c^2 \rho_{\text{l}}}{8\mu_{\text{l}}} \frac{\Delta P_{\text{l}}}{l_{\text{eff}}} \qquad \text{.....(23)}$$

Relating the heat and mass flows, Q=mL, where L is the latent heat of vaporisation and rearranging:

For porous media, Eq. (23) is usually written:

$$\Delta P_l = \frac{8\mu_l \dot{Q} l_{eff}}{\pi(r_w^2 - r_v^2)\varepsilon r_c^2 \rho_l L} \qquad \text{.....(24)}$$

$$\Delta P_l = \frac{b\mu_l \dot{Q} l_{eff}}{\pi(r_w^2 - r_v^2)\varepsilon r_c^2 \rho_l L} \qquad \text{.....(25)}$$

The numerical coefficient 8, derived for round tubes earlier, is replaced by the dimensionless constant, b, typically 10 <b < 20 to include a correction for tortuosity.

Whilst this relation can be useful for a theoretical treatment, it contains three constants, b, ε and r_c, which are all difficult to measure in practice. It is therefore useful to relate the pressure drop and flow rate for a wick structure by using a form of Darcy's 'Law':

$$\Delta P_l = \frac{\mu_l l_{eff} \dot{m}}{\rho_l K A} \qquad \text{.....(26)}$$

where K is the wick permeability. Comparison of Eq. (25) with Eq. (26) shows that Darcy's 'Law' is the Hagen Poiseuille equation with correction terms included in the constant K to take account of pore size, pore distribution and tortuosity. It serves to provide a definition of permeability, K, a quantity which can be easily measured.

4.6. Vapour phase pressure difference ΔP_v

4.6.1. Introduction

The total vapour phase difference in pressure will be the sum of the pressure drops in the three regions of a heat pipe, namely the evaporator drop ΔP_{ve}, the adiabatic section drop ΔP_{va}, and the pressure drop in the condensing region ΔPvc. The problem of calculating the vapour pressure drop is complicated in the evaporating and condensing regions by radial flow due to evaporation or condensation. It is convenient to define a further Reynolds number, the radial Reynolds number:

$$Re_r = \frac{\rho_v v_r r_v}{\mu_v}$$

to take account of the radial velocity component v_r at the wick where $r = r_v$.

By convention the vapour space radius r_v is used rather than the vapour space diameter which is customary in the definition of axial Reynolds number. Re_r is positive in the evaporator section and negative in the condensing section. In most practical heat pipes Re_r lies in the range of 0.1-100.

Rer is related to the radial rate of mass injection or removal per unit length $(d\dot{m}/dz)$ as follows:

$$Re_r = \frac{1}{2\pi\mu_v}\frac{d\dot{m}}{dz}$$

Figure 8 taken from Busse [6], shows Re_r as a function of power/unit length for various liquid metal working fluids. Clearly, the kinetic head may be a significant component of the vapour pressure drop in the evaporator, and result in an appreciable pressure rise in the condenser when working with liquid metals.

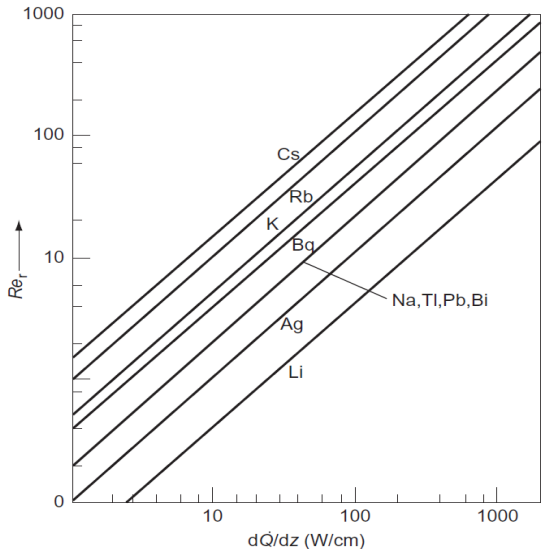

Figure 8

4.6.2. Incompressible flow: simple one-dimensional theory

In the following treatment we will regard the vapour as an incompressible fluid. This assumption implies that the flow velocity v is small compared to the velocity of sound c, in the vapour, i.e. the Mach number:

$$\frac{v}{c} < 0.3$$

Alternatively, this condition implies that the treatment is valid for heat pipes in which ΔP_v is small compared with P_v, the average vapour pressure in the pipe. This assumption is not necessarily valid during start-up, nor is it always true in the case of high-temperature liquid metal heat pipes. The effect of compressibility of the vapour is considered later in the report.

In the evaporator region the vapour pressure gradient will be necessary to carry out two functions.

i. To accelerate the vapour entering the evaporator section up to the axial velocity v. Since, on entering the evaporator, this vapour will have radial velocity but no axial velocity. The necessary pressure gradient we will call the inertial term $\Delta P'_v$.
ii. To overcome frictional drag forces at the surface $r=r_v$ at the wick. This is the viscous term $\Delta P''_v$.

We can estimate the magnitude of the inertial term as follows. If the mass flow/unit area of cross section at the evaporator is ρv then the corresponding momentum flux/ unit will be given by ρv^2. This momentum flux in the axial direction must be provided by the inertial term of the pressure gradient. Hence:

$$\Delta P'_v = \rho v^2$$

Note that $\Delta P'_v$ is independent of the length of the evaporator section. The way in which $\Delta P'_v$ varies along the length of the evaporator is shown in Fig. 9(a). If we assume laminar flow, we can estimate the viscous contribution to the total evaporator pressure loss by integrating the Hagen -Poiseuille equation. If the rate of mass entering the evaporator per unit length dm/dz is constant we find by integrating the mass equation along the length of the evaporator section:

$$\Delta P''_v = \frac{8\mu_v \dot{m} l_e}{\rho_v \pi r_v^4} \frac{1}{2}$$

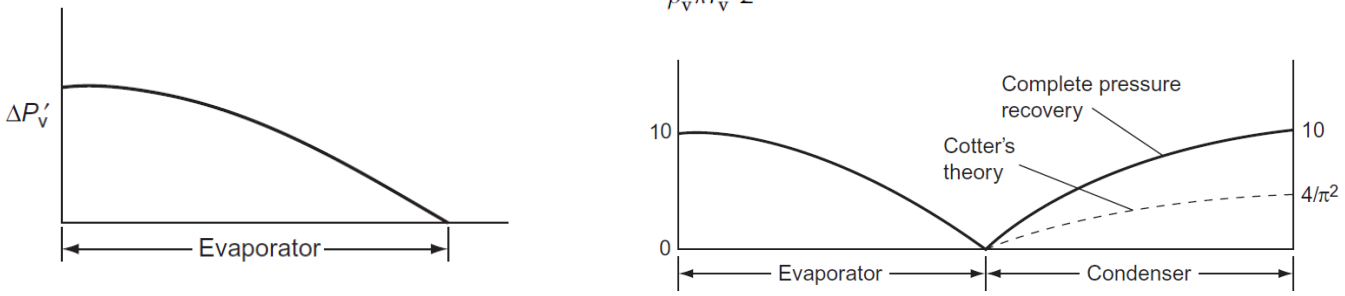

Figure 9a(left) and 9b(right)

$$\Delta P_{ve} = \Delta P'_v + \Delta P''_v$$
$$\Delta P_{ve} = \rho v^2 + \frac{8\mu_v \dot{m} l_e}{\rho \pi r_v^4} \frac{1}{2}$$

Thus the total pressure drop in the evaporator region ΔP_{ve} will be given by the sum of the two terms:

The condenser region may be treated in a similar manner, but in this case axial momentum will be lost as the vapour stream is brought to rest so the inertial term will be negative, that is there will be pressure recovery. For the simple theory the two inertial terms will cancel and the total pressure drop in the vapour phase will be due entirely to the viscous terms. However, it is not always possible to recover the initial pressure term in the condensing region. In the adiabatic section the pressure difference will contain only the viscous term which will be given either by the Hagen-Poiseuille equation or the Fanning equation depending on whether the flow is laminar or turbulent.

By Cotter and Busse theory, the modified pressure drop equations are, including losses in pressure recovery:

For laminar flow:

$$\Delta P_v = \left(1 - \frac{4}{\pi^2}\right) \frac{\dot{m}}{8\rho_v r_v^4} + \frac{8\mu_v \dot{m} l_a}{\pi \rho_v r_v^4} \qquad \text{.....(27)}$$

For turbulent flow:

$$\Delta P_{va} = \frac{2}{r_v} f \frac{1}{2} \rho_v v^2 l_a \quad Re > 2100 \qquad \text{.....(28)}$$

4.6.3. Pressure recovery

The pressure drop in the evaporator and condenser regions consists of two terms, an inertial term and a term due to viscous forces. Simple theory suggests that the inertial term will have the opposite sign in the condenser region and should cancel out that of the evaporator (Fig. 9(b)). There is experimental evidence for this pressure recovery. Grover et al. [7]provided an impressive demonstration with a sodium heat pipe. In these experiments they achieved 60% pressure recovery. The radial Reynolds number was greater than 10. For simplicity in Fig. 9(b) the viscous component of pressure drop has been omitted. The liquid pressure drop is also shown in Fig. 10(a) (c). Ernst [8] has pointed out that if the pressure recovery in the condenser region is greater than the liquid pressure drop, Fig. 10(b), then the meniscus in the wick will be convex. Whilst this is possible in principle, under normal heat pipe operation there is excess in the condenser region so that this condition cannot occur.

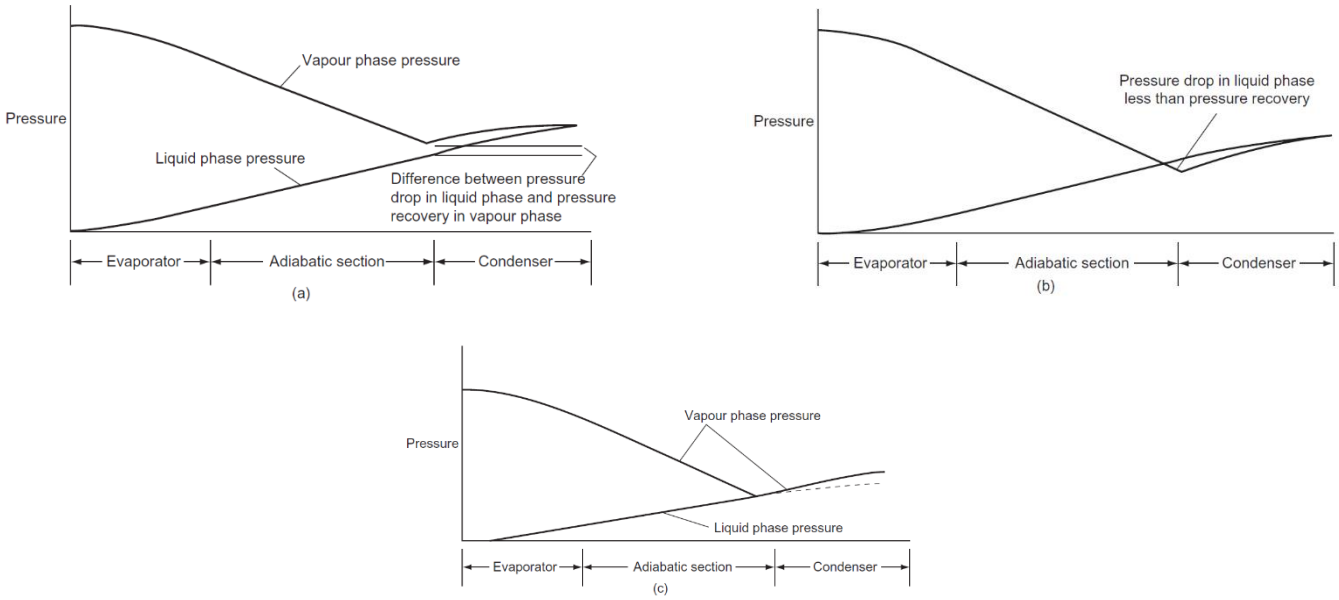

Figure 10

4.6.4. Two-dimensional incompressible flow

The previous discussion has been restricted to one dimensional flow. In practical heat pipes the temperature and pressure are not constant across the cross section and this variation is particularly important in the condenser region. A number of authors have considered this two dimensional- problem. Bankston and Smith [9]have solved the Navier-Stokes equation by numerical methods. Bankston and Smith showed that axial velocity reversal occurred at the end of the condenser section under conditions of high evaporation and condensation rates. In spite of this extreme divergence from the assumption of uniform flow, one-dimensional analyses yield good results for a particular range of Reynolds Numbers. This is illustrated in Fig. 11.

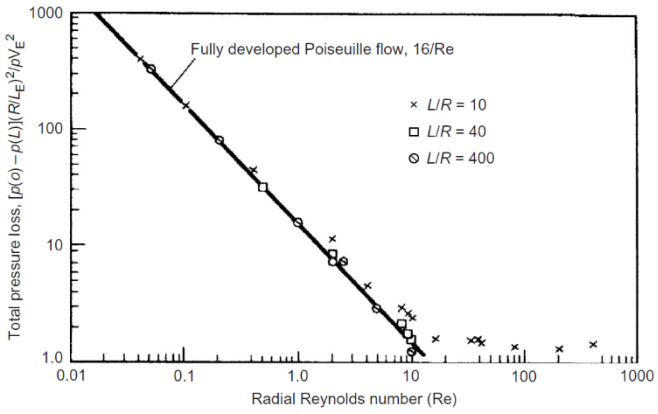

Figure 11

4.6.5. Compressible flow

In a cylindrical heat pipe the axial mass flow increases along the length of the evaporator region to a maximum value at the end of the evaporator; it will then decrease along the condenser region. The flow velocity will rise to a maximum value at the end of the evaporator region where the pressure will have fallen to a minimum. Deverall et al. [10] have drawn attention to the similarity in flow behaviour between such a heat pipe and that of a gas flowing through a converging-diverging nozzle. In the former the area remains constant but the mass flow varies, whereas in the latter the mass flow is constant but the cross-sectional area is changed. It is helpful to examine the behaviour of the convergent-divergent nozzle

in more detail before returning to the heat pipe. Let the pressure of the gas at the entry to the nozzle be kept constant and consider the effect of reducing the pressure at the outlet. With reference to the curves in Fig. 2.18 we can see the effect of increasing the flow through a nozzle. For the flow of Curve A, the pressure difference between inlet and outlet is small. The gas velocity will increase to a maximum value in the position of minimum cross section, or throat, falling again in the divergent region. The velocity will not reach the sonic value. The pressure passes through a minimum in the throat. If the outlet pressure is now reduced the flow will increase and the situation shown in Curve B can be attained. Here the velocity will increase through the convergent region, rising to the sonic velocity in the throat. As before, the velocity will reduce during travel through the diverging section and there will be some pressure recovery. If the outlet pressure is further reduced the flow rate will remain constant and the pressure profile will follow Curve C. The gas will continue to accelerate after entering the divergent region and will become supersonic. Pressure recovery will occur after a shock front. Curve D shows that for a certain exit pressure the gas can be caused to accelerate throughout the diverging region. Further pressure reduction will not affect the flow pattern in the nozzle region. It should be noted that after Curve C pressure reduction does not affect the flow pattern in the converging section, hence the mass flow does not increase after the throat velocity has attained the sonic value. This condition is referred to as choked flow.

Deverall et al. have shown that a simple one-dimensional model provides a good description of the compressible flow behaviour. Consider the evaporator section using the nomenclature of Fig. 12. The pressure $P_1 = P_o$, where P_o is the stagnation pressure of the fluid.

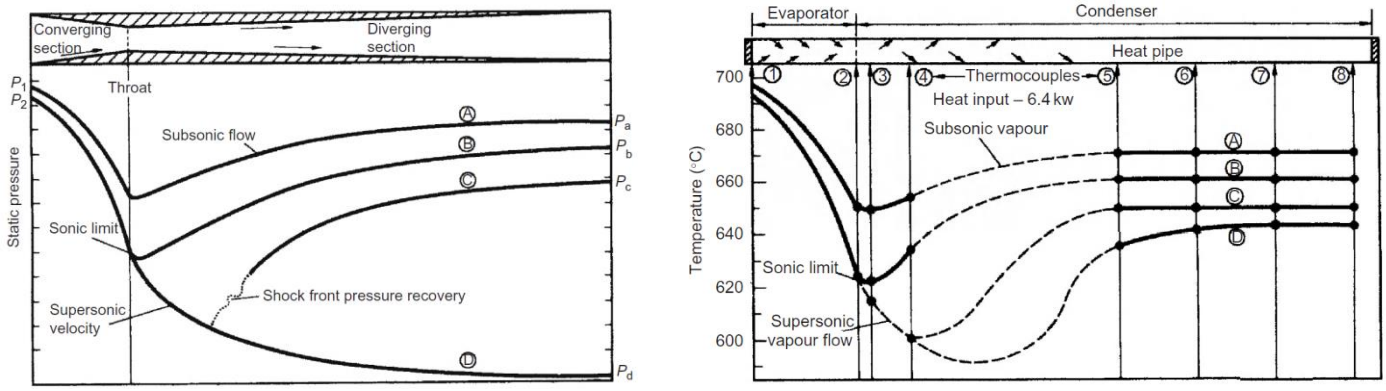

Figure 12

4.7. Entrainment

In a heat pipe the vapour flows from the evaporator to the condenser and the liquid is returned by the wick structure. At the interface between the wick surface and the vapour the latter will exert a shear force on the liquid in the wick. The magnitude of the shear force will depend on the vapour properties and velocity and its action will be to entrain droplets of liquid and transport them to the condenser end. This tendency to entrain is resisted by the surface tension in the liquid. Entrainment will prevent the heat pipe operating and represents one limit to performance.

The Weber number, We, which is representative of the ratio between inertial vapour forces and liquid surface tension forces, provides a convenient measure of the likelihood of entrainment. The Weber number is defined as:

$$We = \frac{\rho_v v^2 z}{2\pi\sigma_l} \qquad \text{.....(28)}$$

where ρ_v is the vapour density, v is the vapour velocity, σ_l is surface tension and z is a dimension characterising the vapour-liquid surface. In a wicked heat pipe z is related to the wick spacing.

It may be assumed that entrainment may occur when We is of the order 1. The limiting vapour velocity, vc, is thus given by:

$$v_c = \sqrt{\frac{2\pi\sigma_l}{\sigma_v z}} \qquad \text{.....(29)}$$

and, relating the axial heat flux to the vapour velocity, we get the entrainment limit :

$$\dot{q} = \sqrt{\frac{2\pi\rho_v L^2 \sigma_l}{z}} \qquad \text{.....(30)}$$

Extracting the fluid properties from Eq. (30) suggests as a suitable figure of merit for working fluids from the point of view of entrainment. Cheung [11] has plotted this figure of merit against temperature for a number of liquid metals, and this is reproduced as Fig. 13.

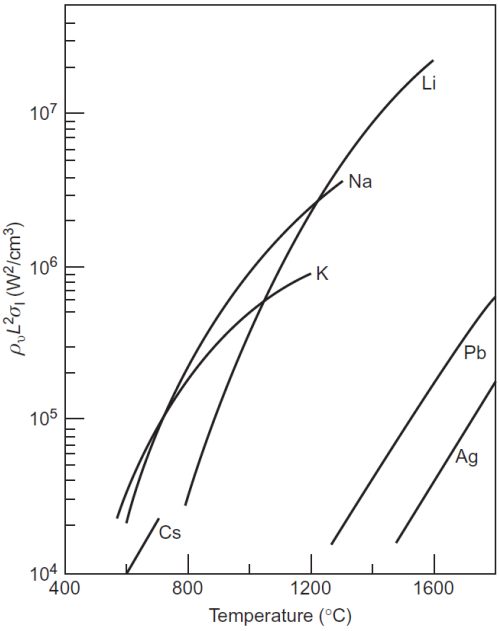

Figure 13

4.8. Heat transfer and temperature difference

4.8.1. Introduction

The transfer of heat and the associated temperature drops in a heat pipe is discussed below. The latter can be represented by thermal resistances and an equivalent circuit is shown in Fig. 14. Heat can both enter and leave the heat pipe by conduction from a heat source/sink, by convection or by thermal radiation. The pipe may also be heated by eddy currents or by electron bombardment, and cooled by electron emission. Further temperature drops will occur by thermal conduction through the heat pipe walls at both the evaporator and condenser regions. The temperature drops through the wicks arise in several ways. It is found that a thermal resistance exists at the two vapour liquid surfaces and also in the vapour column.

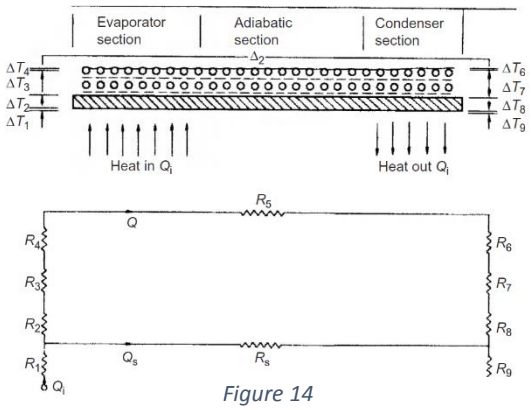

Figure 14

4.8.2. Heat transfer in the evaporator region

For low values of heat flux the heat will be transported to the liquid surface partly by conduction through the wick and liquid and partly by natural convection. Evaporation will be from the liquid surface. As the heat flux is increased the liquid in contact with the wall will become progressively superheated and bubbles will form at nucleation sites. These bubbles will transport some energy to the surface by latent heat of vaporisation and will also greatly increase convective heat transfer. With further increase of flux a critical value will be reached, burnout, at which the wick will dry out and the heat pipe will cease to operate.

4.8.3. Boiling heat transfer from plane surfaces

In 1934 Nukiyama [12] performed a pool boiling experiment, passing an electric current through a platinum wire immersed in water. The heat flux was controlled by the current through and voltage across the wire and the temperature of the wire was determined from its resistance. Similar results are obtained when boiling from a plane surface or from the surface of a cylinder. Nukiyama then proposed a boiling curve of the form shown in Fig. 15. This again, forms the basis of all the equations and phenomenon in the heat pipe.

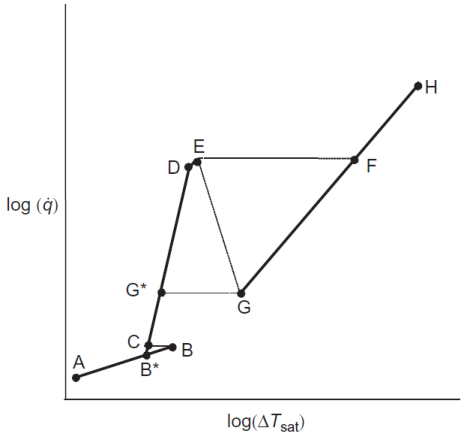

Figure 15

It has been observed that nucleation occurs in cavities within the surface; these cavities contain minute bubbles of trapped gas or vapour which act as starting points for bubble growth. This is illustrated schematically in Fig. 16. When the bubble leaves the site a small bubble remains in the cavity which acts as the start for the next bubble. Consideration of idealised nucleation sites allows some indication of their necessary size if they are to play a part in boiling, with reference to an idealised

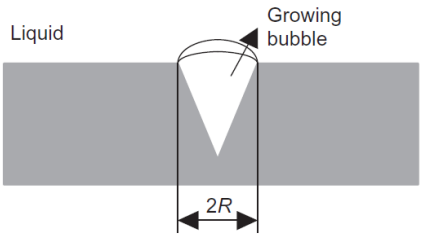

Figure 16

conical cavity as shown in Fig. 16.

The pressure, PB, inside a bubble is somewhat higher than the pressure in the surrounding liquid:

$$P_B = P + \frac{2\sigma_l}{R}$$

where P is the liquid pressure, r is the radius of curvature of the bubble and σ_l is the surface tension of the liquid. The radius of curvature is a maximum when the bubble forms a hemispherical cap over the cavity, i.e. r= R, the radius of the mouth of the cavity. This is the condition for PB to be a maximum. If the bubble is to grow then the wall temperature must be sufficiently high to vaporise the liquid at a pressure PB. In order for the bubble to grow:

The Clapeyron equation states that the slope of the vapour pressure curve is given by:

$$T_W > T_{sat} + \frac{dT}{dP}(P_B - P)$$

$$\frac{dP}{dT} = \frac{L}{(v_v - v_l)T_{sat}}$$

Hence, for the bubble to grow:

$$T_W > T_{sat} + \frac{2\sigma_l}{R}\frac{v_v T_{sat}}{L} = \frac{2\sigma_l}{R}\frac{\Delta T_{sat}}{\rho_v L} \qquad \text{.....(31)}$$

The radius of the cavity and the superheat, ΔTsat, at which nucleation from the cavity starts, can be related as:

$$R = \frac{2\sigma_l T_{sat}}{L\rho_v \Delta T_{sat}} \qquad \text{.....(32)}$$

Hsu [13] has conducted a more rigorous analysis and showed that

$$\Delta T = \frac{3.06\sigma_l T_{sat}}{\rho_v L\delta} \qquad \text{.....(33)}$$

where δ is the thermal boundary layer thickness, as a first approximation this may be taken as the average diameter of cavities on the surface. For typical heat pipe evaporators this is approximately 25 μm. This must be high for the working fluid.

As for nucleate boiling the critical peak flux or boiling crisis flux is also very dependent on surface conditions. For water at atmospheric pressure the peak flux lies in the range 130950 kW/m2 and this is between 3 and 8 times the value obtained for organic liquids. The corresponding temperature difference for both water and organics is between 20°C and 50°C. Liquid metals have the advantage of low viscosity and high thermal conductivity and the alkali metals in the pressure range 0.110 bar give peak flux values of 100300 kW/m² with a corresponding temperature difference of around 5°C. A number of authors have provided relationships to enable the critical heat flux $\dot{q}_{cr}$ to be predicted. One of these was developed by Rohsenow and Griffith [14] who obtained the following expression:

$$\dot{q}_{cr} = 0.012 L\rho_v \left[\frac{\rho_l - \rho_v}{\rho_v}\right]^{0.6} \qquad \text{.....(34)}$$

This is the burnout limit.

4.8.4. Wick thermal conductivity

The effective conductivity of the wick saturated with the working fluid is required for calculating the thermal resistance of the wick at the condenser region and also, under conditions of evaporation when the evaporation is from the surface for the evaporator region. Two models are used in the literature (see also Chapter 3).

i. Parallel case: Here it is assumed that the wick and working fluid are effectively in parallel .If k_l is the thermal conductivity of the working fluid and k_s is the thermal conductivity of the wick material and

$$k_w = (1-\varepsilon)k_s + \varepsilon k_l \qquad \varepsilon = \text{Voidage fraction} = \frac{\text{Volume of working fluid in wick}}{\text{Total volume of wick}}$$

.....(35)

ii. Series case: If the two materials are assumed to be in series.

$$k_w = \frac{1}{((1-\varepsilon)/k_s) + (\varepsilon/k_l)} \qquad \text{.....(36)}$$

Additionally, convection currents in the wick will tend to increase the effective thermal conductivity.

5. Assumptions and relaxations considered

The entire program is constructed based on several assumptions and relaxations, with respect to the governing equations, fluids and materials considered. These are listed below for clarity and for the sake of avoiding any errors/miscommunications pertaining to the aim of this project.

- The fluid and vapour streams are modelled as one dimensional plug flows
- The heat transfer is primarily through the main surface, including the wick. Hence axial losses etc. is neglected
- Fluid mal-distribution, if it somehow exists, is neglected
- The heat pipe is assumed to be completely insulated from the surroundings, except for the condenser part
- The fluid thermo physical properties are considered at the two temperatures for calculations, viz. the evaporator and condenser temperatures
- The governing equations, including the sonic limit, boiling limit, entrainment limit each have their own assumptions, as clearly stated in the basic theory and working principles
- The specific power output is given, assuming that fluid at the ambient temperature is made to flow over the circular circumferential area of the condenser
- The thermo-physical properties of the fluids are obtained at different temperatures by extrapolating values linearly in between set points, where the values have already been fed
- The total number of fluids considered for the design phase are 16 in number, and 7 materials are chosen, for both wick and the wall
- Materials are selected strictly based on the compatibility chart, as given in Appendix, and not based on specific applications (such as Aluminium for Aerospace etc.)
- Fluids are selected from a table that mentions its operating ranges, with a tolerance of ± 5 ^{o}C
- Incompressibility of the fluid and vapour is assumed, with a system of checks and measures (by specifying the sonic limit), and so start-up problems are not considered
- Only homogenous wicks are considered for the design of heat pipes in the software
- Materials considered for the wick and the walls are the same, hence multiple(and unwanted) possibilities are omitted from the results
- Wick materials are hence generalised, and specific material types are not chosen – that is variation that can exist in the material is neglected. A standard grid size is assumed by default.
- Standard values of parameters are taken if the user does not specify any input, say for example , the area considerations

6. Design Process

6.1. Basic procedure: Selection of Fluid and Pipe material

Step 1: For the given Temperature range, list out all the compatible fluids from the charts in Appendix

Step 2: Eliminate the fluids whose Sonic Limit Heat Flux are lesser than actual heat flux due to the heating element.

$$\dot{q}_s = \rho_v L \sqrt{\frac{\gamma R T_v}{2(\gamma+1)}} \qquad \text{where} \qquad R = \frac{R_o}{\text{Molecular weight}} = \frac{8315}{M_w} \text{ J/kg K}$$

Step 3: Eliminate the fluids whose maximum heat transfer due to entrainment is less than heat generated by heating element.

$$\dot{Q}_{ent} = \pi r_v^2 L \sqrt{\frac{2\pi\rho_v\sigma_l}{z}}$$

Step 4: Select the fluids with the best Merit No. and the maximum Degree of Superheat.

$$\text{Merit No.} = \rho_l \frac{\sigma_l L}{\mu_l} \qquad \text{and} \qquad \Delta T = \frac{3.06\sigma_l T_{sat}}{\rho_v L\delta}$$

Step 5: For the selected Fluids list out all compatible pipe materials from the charts in Appendix.

Step 6: Calculate the required Wall thickness to withstand the vapour pressure of the corresponding fluid for all the compatible materials.

$$t = \frac{Pr}{\Omega}$$

Step 7: Select the wall material which has the least mass penalty.

6.2. Detail design

Step 1: Solve for the wick area by equating the Capillary Pressure Drop to Total Pressure Drop which includes liquid, vapour and gravitational pressure drop.

$$\Delta P_v = \left(1 - \frac{4}{\pi^2}\right)\frac{\dot{m}}{8\rho_v r_v^4} + \frac{8\mu_v \dot{m} l_a}{\pi\rho_v r_v^4} \qquad \Delta P_l = \frac{\mu_l \dot{Q} l_{eff}}{\rho_l L A_w K} \qquad \Delta P_g = \rho_l g h \qquad \Delta P_c = \frac{2\sigma_l \cos\theta}{r_e}$$

Solve for A_w which is the only unknown. Since $A_w = \pi(r_w^2 - r_v^2)$, find the thickness of the wick required.

Step 2: Calculate the Heat transfer Coefficient at the condenser using heat balancing equation at the condenser side.

Step 3: Calculate the corresponding Reynolds no. and hence the speed of the fluid jet to cause the cooling in condenser.

Step 4: Calculate the Specific Power of the Fan to generate the fluid jet speed.

7. Pseudo-Code

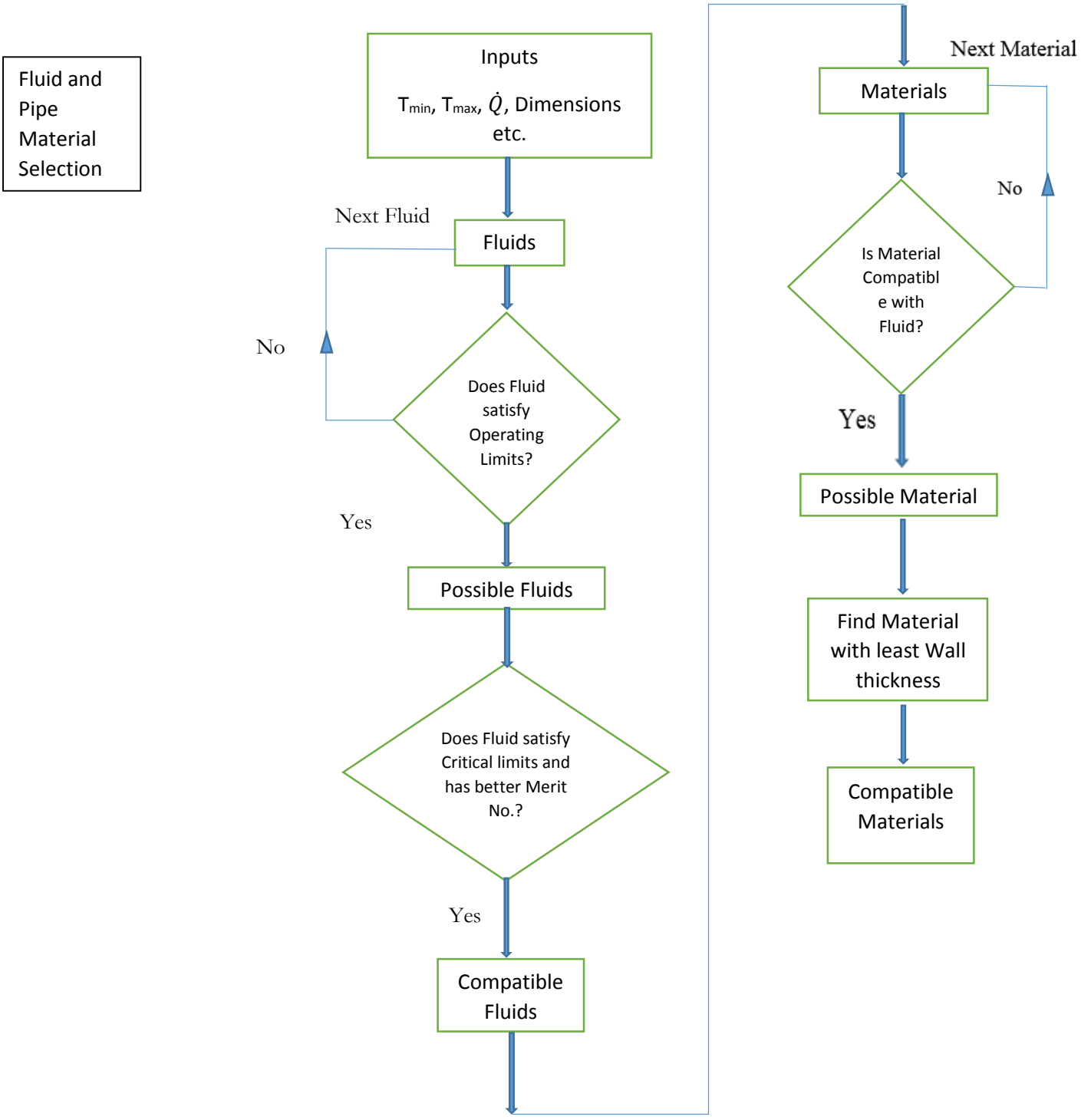

8. Data-Tables

Given below is the data utilized in the MATLAB code. Few points to be noted:

- All properties were converted into matrices using the *uiimport* command
- Values not given in the tables have been linearly interpolated as it would be done for manual calculations
- Surface tension values for high temperature fluids have been taken to be 0 due to lack of data in literature

Thermo-Physical Properties of Selected Working Fluids

Helium

Temperature(^{0}C)	Latent heat (kJ/kg)	Liquid Density (kg/m^3)	Vapour Density (kg/m^3)	Liquid Thermal Conductivity (W/mK)	Liquid Viscosity (cP)	Vapour Viscosity (cP x 10^2)	Vapour Pressure (bar)	Vapour Specific Heat (kJ/kg K)	Liquid Surface Tension (N/m x 10^2)
-271	22.8	148.3	26	1.81	3.9	0.2	0.06	2.045	0.26
-270	23.6	140.7	17	2.24	3.7	0.3	0.32	2.699	0.19
-269	20.9	128	10	2.77	2.9	0.6	1	4.619	0.09
-268	4	113.8	8.5	3.5	1.34	0.9	2.29	6.642	0.01

Nitrogen

Temperature(^{0}C)	Latent heat (kJ/kg)	Liquid Density (kg/m^3)	Vapour Density (kg/m^3)	Liquid Thermal Conductivity (W/mK)	Liquid Viscosity (cP)	Vapour Viscosity (cP x 10^2)	Vapour Pressure (bar)	Vapour Specific Heat (kJ/kg K)	Liquid Surface Tension (N/m x 10^2)
-203	210	830	1.84	0.15	0.248	0.48	0.48	1.083	1.054
-200	205.5	818	3.81	0.146	0.194	0.51	0.74	1.082	0.985
-195	198	798	7.1	0.139	0.151	0.56	1.62	1.079	0.87
-190	190.5	778	10.39	0.132	0.126	0.6	3.31	1.077	0.766
-185	183	758	13.68	0.125	0.108	0.65	4.99	1.074	0.662
-180	173.7	732	22.05	0.117	0.095	0.71	6.69	1.072	0.561
-175	163.2	702	33.8	0.11	0.086	0.77	8.37	1.07	0.464
-170	152.7	672	45.55	0.103	0.08	0.83	1.07	1.068	0.367
-160	124.2	603	80.9	0.089	0.072	1	19.37	1.063	0.185
-150	66.8	474	194	0.075	0.065	1.5	28.8	1.059	0.11

Ammonia

Temperature(^{0}C)	Latent heat (kJ/kg)	Liquid Density (kg/m^3)	Vapour Density (kg/m^3)	Liquid Thermal Conductivity (W/mK)	Liquid Viscosity (cP)	Vapour Viscosity (cP x 10^2)	Vapour Pressure (bar)	Vapour Specific Heat (kJ/kg K)	Liquid Surface Tension (N/m x 10^2)
-60	1343	714.4	0.03	0.294	0.36	0.72	0.27	2.05	4.062
-40	1384	690.4	0.05	0.303	0.29	0.79	0.76	2.075	3.574
-20	1338	665.5	1.62	0.304	0.26	0.85	1.93	2.1	3.09
0	1263	638.6	3.48	0.298	0.25	0.92	4.24	2.125	2.48
20	1187	610.3	6.69	0.286	0.22	1.01	8.46	2.15	2.133
40	1101	579.5	12	0.272	0.2	1.16	15.34	2.16	1.833
60	1026	545.2	20.49	0.255	0.17	1.27	29.8	2.18	1.367
80	891	505.7	34.13	0.235	0.15	1.4	40.9	2.21	0.767
100	699	455.1	54.92	0.212	0.11	1.6	63.12	2.26	0.5
120	428	374.4	113.16	0.184	0.07	1.89	90.44	2.292	0.15

Pentane

Temperature(^{0}C)	Latent heat (kJ/kg)	Liquid Density (kg/m^3)	Vapour Density (kg/m^3)	Liquid Thermal Conductivity (W/mK)	Liquid Viscosity (cP)	Vapour Viscosity (cP x 10^2)	Vapour Pressure (bar)	Vapour Specific Heat (kJ/kg K)	Liquid Surface Tension (N/m x 10^2)
-20	390	663	0.01	0.149	0.344	0.51	0.1	0.825	2.01
0	378.3	644	0.75	0.143	0.283	0.53	0.24	0.874	1.79
20	366.9	625.5	2.2	0.138	0.242	0.58	0.76	0.922	1.58
40	355.5	607	4.35	0.133	0.2	0.63	1.52	0.971	1.37
60	342.3	585	6.51	0.128	0.174	0.69	2.28	1.021	1.17
80	329.1	563	10.61	0.127	0.147	0.74	3.89	1.05	0.97
100	295.7	537.6	16.54	0.124	0.128	0.81	7.19	1.088	0.83
120	269.7	509.4	25.2	0.122	0.12	0.9	13.81	1.164	0.6

Acetone

Temperature(^{0}C)	Latent heat (kJ/kg)	Liquid Density (kg/m^3)	Vapour Density (kg/m^3)	Liquid Thermal Conductivity (W/mK)	Liquid Viscosity (cP)	Vapour Viscosity (cP x 10^2)	Vapour Pressure (bar)	Vapour Specific Heat (kJ/kg K)	Liquid Surface Tension (N/m x 10^2)
-40	660	860	0.03	0.2	0.8	0.68	0.01	2	3.1
-20	615.6	845	0.1	0.189	0.5	0.73	0.03	2.06	2.76
0	564	812	0.26	0.183	0.395	0.78	0.1	2.11	2.62
20	552	790	0.64	0.181	0.323	0.82	0.27	2.16	2.37
40	536	768	1.05	0.175	0.269	0.86	0.6	2.22	2.12
60	517	744	2.37	0.168	0.226	0.9	1.15	2.28	1.86
80	495	719	4.3	0.16	0.192	0.95	2.15	2.34	1.62
100	472	689.6	6.94	0.148	0.17	0.98	4.43	2.39	1.34
120	426.1	660.3	11.02	0.135	0.148	0.99	6.7	2.45	1.07
140	394.4	631.8	18.61	0.126	0.132	1.03	10.49	2.5	0.81

Methanol

Temperature(^{0}C)	Latent heat (kJ/kg)	Liquid Density (kg/m^3)	Vapour Density (kg/m^3)	Liquid Thermal Conductivity (W/mK)	Liquid Viscosity (cP)	Vapour Viscosity (cP x 10^2)	Vapour Pressure (bar)	Vapour Specific Heat (kJ/kg K)	Liquid Surface Tension (N/m x 10^2)
-50	1194	843.5	0.01	0.21	1.7	0.72	0.01	1.2	3.26
-30	1187	833.5	0.01	0.208	1.3	0.78	0.02	1.27	2.95
-10	1182	818.7	0.04	0.206	0.945	0.85	0.04	1.34	2.63
10	1175	800.5	0.12	0.204	0.701	0.91	0.1	1.4	2.36
30	1155	782	0.31	0.203	0.521	0.98	0.25	1.47	2.18
50	1125	764.1	0.77	0.202	0.399	1.04	0.55	1.54	2.01
70	1085	746.2	1.47	0.201	0.314	1.11	1.31	1.61	1.85
90	1035	724.4	3.01	0.199	0.259	1.19	2.69	1.79	1.66
110	980	703.6	5.64	0.197	0.211	1.26	4.98	1.92	1.46
130	920	685.2	9.81	0.195	0.166	1.31	7.86	1.92	1.25
150	850	653.2	15.9	0.193	0.138	1.38	8.94	1.92	1.04

Flutec PP2

Temperature(^{0}C)	Latent heat (kJ/kg)	Liquid Density (kg/m^3)	Vapour Density (kg/m^3)	Liquid Thermal Conductivity (W/mK)	Liquid Viscosity (cP)	Vapour Viscosity (cP x 10^2)	Vapour Pressure (bar)	Vapour Specific Heat (kJ/kg K)	Liquid Surface Tension (N/m x 10^2)
-30	106.2	1942	0.13	0.637	5.2	0.98	0.01	0.72	1.9
-10	103.1	1886	0.44	0.626	3.5	1.03	0.02	0.81	1.71

10	99.8	1829	1.39	0.613	2.14	1.07	0.09	0.92	1.52
30	96.3	1773	2.96	0.601	1.435	1.12	0.22	1.01	1.32
50	91.8	1716	6.43	0.588	1.005	1.17	0.39	1.07	1.13
70	87	1660	11.79	0.575	0.72	1.22	0.62	1.11	0.93
90	82.1	1599	21.99	0.563	0.543	1.26	1.43	1.17	0.73
110	76.5	1558	34.92	0.55	0.429	1.31	2.82	1.25	0.52
130	70.3	1515	57.21	0.537	0.314	1.36	4.83	1.33	0.32
160	59.1	1440	103.63	0.518	0.167	1.43	8.76	1.45	0.01

Ethanol

Temperature(^{0}C)	Latent heat (kJ/kg)	Liquid Density (kg/m^3)	Vapour Density (kg/m^3)	Liquid Thermal Conductivity (W/mK)	Liquid Viscosity (cP)	Vapour Viscosity (cP x 10^2)	Vapour Pressure (bar)	Vapour Specific Heat (kJ/kg K)	Liquid Surface Tension (N/m x 10^2)
-30	939.4	825	0.02	0.177	3.4	0.75	0.01	1.25	2.76
-10	928.7	813	0.03	0.173	2.2	0.8	0.02	1.31	2.66
10	904.8	798	0.05	0.17	1.5	0.85	0.03	1.37	2.57
30	888.6	781	0.38	0.168	1.02	0.91	0.1	1.44	2.44
50	872.3	762.2	0.72	0.166	0.72	0.97	0.29	1.51	2.31
70	858.3	743.1	1.32	0.165	0.51	1.02	0.76	1.58	2.17
90	832.1	725.3	2.59	0.163	0.37	1.07	1.43	1.65	2.04
110	786.6	704.1	5.17	0.16	0.28	1.13	2.66	1.72	1.89
130	734.4	678.7	9.25	0.159	0.21	1.18	4.3	1.78	1.75

Heptane

Temperature(^{0}C)	Latent heat (kJ/kg)	Liquid Density (kg/m^3)	Vapour Density (kg/m^3)	Liquid Thermal Conductivity (W/mK)	Liquid Viscosity (cP)	Vapour Viscosity (cP x 10^2)	Vapour Pressure (bar)	Vapour Specific Heat (kJ/kg K)	Liquid Surface Tension (N/m x 10^2)
-20	384	715.5	0.01	0.143	0.69	0.57	0.01	0.83	2.42
0	372.6	699	0.17	0.141	0.53	0.6	0.02	0.87	2.21
20	362.2	683	0.49	0.14	0.43	0.63	0.08	0.92	2.01
40	351.8	667	0.97	0.139	0.34	0.66	0.2	0.97	1.81
60	341.5	649	1.45	0.137	0.29	0.7	0.32	1.02	1.62
80	331.2	631	2.31	0.135	0.24	0.74	0.62	1.05	1.43
100	319.6	612	3.71	0.133	0.21	0.77	1.1	1.09	1.28
120	305	592	6.08	0.132	0.18	0.82	1.85	1.16	1.1

Water

Temperature(^{0}C)	Latent heat (kJ/kg)	Liquid Density (kg/m^3)	Vapour Density (kg/m^3)	Liquid Thermal Conductivity (W/mK)	Liquid Viscosity (cP)	Vapour Viscosity (cP x 10^2)	Vapour Pressure (bar)	Vapour Specific Heat (kJ/kg K)	Liquid Surface Tension (N/m x 10^2)
20	2448	998.2	0.02	0.603	1	0.96	0.02	1.81	7.28
40	2402	992.3	0.05	0.63	0.65	1.04	0.07	1.89	6.96
60	2359	983	0.13	0.649	0.47	1.12	0.2	1.91	6.62
80	2309	972	0.29	0.668	0.36	1.19	0.47	1.95	6.26
100	2258	958	0.6	0.68	0.28	1.27	1.01	2.01	5.89
120	2200	945	1.12	0.682	0.23	1.34	2.02	2.09	5.5
140	2139	928	1.99	0.683	0.2	1.41	3.9	2.21	5.06
160	2074	909	3.27	0.679	0.17	1.49	6.44	2.38	4.66
180	2003	888	5.16	0.669	0.15	1.57	10.04	2.62	4.29

200	1967	865	7.87	0.659	0.14	1.65	16.19	2.91	3.89

Flutec PP9

Temperature(^{0}C)	Latent heat (kJ/kg)	Liquid Density (kg/m^3)	Vapour Density (kg/m^3)	Liquid Thermal Conductivity (W/mK)	Liquid Viscosity (cP)	Vapour Viscosity (cP x 10^2)	Vapour Pressure (bar)	Vapour Specific Heat (kJ/kg K)	Liquid Surface Tension (N/m x 10^2)
-30	103	2098	0.01	0.06	5.77	0.82	0	0.8	2.36
0	98.4	2029	0.01	0.059	3.31	0.9	0	0.87	2.08
30	94.5	1960	0.12	0.057	1.48	1.06	0.01	0.94	1.8
60	90.2	1891	0.61	0.056	0.94	1.18	0.03	1.02	1.52
90	86.1	1822	1.93	0.054	0.65	1.21	0.12	1.09	1.24
120	83	1753	4.52	0.053	0.49	1.23	0.28	1.15	0.95
150	77.4	1685	11.81	0.052	0.38	1.26	0.61	1.23	0.67
180	70.8	1604	25.13	0.051	0.3	1.33	1.58	1.3	0.4
225	59.4	1455	63.27	0.049	0.21	1.44	4.21	1.41	0.01

Mercury

Temperature(^{0}C)	Latent heat (kJ/kg)	Liquid Density (kg/m^3)	Vapour Density (kg/m^3)	Liquid Thermal Conductivity (W/mK)	Liquid Viscosity (cP)	Vapour Viscosity (cP x 10^2)	Vapour Pressure (bar)	Vapour Specific Heat (kJ/kg K)	Liquid Surface Tension (N/m x 10^2)
150	308.8	13230	0.01	9.99	1.09	0.39	0.01	1.04	4.45
250	303.8	12995	0.6	11.23	0.96	0.48	0.18	1.04	4.15
300	301.8	12880	1.73	11.73	0.93	0.53	0.44	1.04	4
350	298.9	12763	4.45	12.18	0.89	0.61	1.16	1.04	3.82
400	296.3	12656	8.75	12.58	0.86	0.66	2.42	1.04	3.74
450	293.8	12508	16.8	12.96	0.83	0.7	4.92	1.04	3.61
500	291.3	12308	28.6	13.31	0.8	0.75	8.86	1.04	3.41
550	288.8	12154	44.92	13.62	0.79	0.81	15.03	1.04	3.25
600	286.3	12054	65.75	13.87	0.78	0.87	23.77	1.04	3.15
650	283.5	11962	94.39	14.15	0.78	0.95	34.95	1.04	3.03
750	277	11800	170	14.8	0.77	1.1	63	1.04	2.75

Caesium

Temperature(^{0}C)	Latent heat (kJ/kg)	Liquid Density (kg/m^3)	Vapour Density (kg/m^3)	Liquid Thermal Conductivity (W/mK)	Liquid Viscosity (cP)	Vapour Viscosity (cP x 10^2)	Vapour Pressure (bar)	Vapour Specific Heat (kJ/kg K)	Liquid Surface Tension (N/m x 10^2)
375	530.4	1740	0.0001	20.76	0.25	2.2	0.02	0.156	5.81
425	520.4	1730	0.0001	20.51	0.23	2.3	0.04	0.156	5.61
475	515.2	1720	0.0002	20.02	0.22	2.4	0.09	0.156	5.36
525	510.2	1710	0.0003	19.52	0.2	2.5	0.16	0.156	5.11
575	502.8	1700	0.0007	18.83	0.19	2.55	0.36	0.156	4.81
625	495.3	1690	0.001	18.13	0.18	2.6	0.57	0.156	4.51
675	490.2	1680	0.0018	17.48	0.17	2.67	1.04	0.156	4.21
725	485.2	1670	0.0026	16.83	0.17	2.75	1.52	0.156	3.91
775	477.8	1655	0.004	16.18	0.16	2.28	2.46	0.156	3.66
825	470.3	1640	0.0055	15.53	0.16	2.9	3.41	0.156	3.41

Potassium

Temperature(^{0}C)	Latent heat (kJ/kg)	Liquid Density (kg/m^3)	Vapour Density (kg/m^3)	Liquid Thermal Conductivity (W/mK)	Liquid Viscosity (cP)	Vapour Viscosity (cP x 10^2)	Vapour Pressure (bar)	Vapour Specific Heat (kJ/kg K)	Liquid Surface Tension (N/m x 10^2)
350	2093	763.1	0.002	51.08	0.21	0.15	0.01	5.32	9.5
400	2078	748.1	0.006	49.08	0.19	0.16	0.01	5.32	9.04
450	2060	735.4	0.015	47.08	0.18	0.16	0.02	5.32	8.69
500	2040	725.4	0.031	45.08	0.17	0.17	0.05	5.32	8.44
550	2020	715.4	0.062	43.31	0.15	0.17	0.1	5.32	8.16
600	2000	705.4	0.111	41.81	0.14	0.18	0.19	5.32	7.86
650	1980	695.4	0.193	40.08	0.13	0.19	0.35	5.32	7.51
700	1969	685.4	0.314	38.08	0.12	0.19	0.61	5.32	7.12
750	1938	675.4	0.486	36.31	0.12	0.2	0.99	5.32	6.72
800	1913	665.4	0.716	34.81	0.11	0.2	1.55	5.32	6.32
850	1883	653.1	1.054	33.31	0.1	0.21	2.34	5.32	5.92

Sodium

Temperature(^{0}C)	Latent heat (kJ/kg)	Liquid Density (kg/m^3)	Vapour Density (kg/m^3)	Liquid Thermal Conductivity (W/mK)	Liquid Viscosity (cP)	Vapour Viscosity (cP x 10^2)	Vapour Pressure (bar)	Vapour Specific Heat (kJ/kg K)	Liquid Surface Tension (N/m x 10^2)
500	4370	828.1	0.003	70.08	0.24	1.8	0.01	0.904	1.51
600	4243	805.4	0.013	64.62	0.21	1.9	0.04	0.904	1.42
700	4090	763.5	0.05	60.81	0.19	2	0.15	0.904	1.33
800	3977	757.3	0.134	57.81	0.18	2.2	0.47	0.904	1.23
900	3913	745.4	0.306	53.35	0.17	2.3	1.25	0.904	1.13
1000	3827	725.4	0.667	49.08	0.16	2.4	2.81	0.904	1.04
1100	3690	690.8	1.306	45.08	0.16	2.5	5.49	0.904	0.95
1200	3577	669	2.303	41.08	0.15	2.6	9.59	0.904	0.86
1300	3477	654	3.622	37.08	0.15	2.7	15.91	0.904	0.77

Lithium

Temperature(^{0}C)	Latent heat (kJ/kg)	Liquid Density (kg/m^3)	Vapour Density (kg/m^3)	Liquid Thermal Conductivity (W/mK)	Liquid Viscosity (cP)	Vapour Viscosity (cP x 10^2)	Vapour Pressure (bar)	Vapour Specific Heat (kJ/kg K)	Liquid Surface Tension (N/m x 10^2)
1030	20500	450	0.005	67	0.24	1.67	0.07	0.532	2.9
1130	20100	440	0.013	69	0.24	1.74	0.17	0.532	2.85
1230	20000	430	0.028	70	0.23	1.83	0.45	0.532	2.75
1330	19700	420	0.057	69	0.23	1.91	0.96	0.532	2.6
1430	19200	410	0.108	68	0.23	2	1.85	0.532	2.4
1530	18900	405	0.193	65	0.23	2.1	3.3	0.532	2.25
1630	18500	400	0.34	62	0.23	2.17	5.3	0.532	2.1
1730	18200	398	0.49	59	0.23	2.26	8.9	0.532	2.05

Operating Ranges of Some Typical Working Fluids

S.No	Medium	Melting Point(^{0}C)	Boiling Point at Atmospheric Pressure (^{0}C)	Minimal Operating temperature (^{0}C)	Maximal Operating Temperature (^{0}C)
1	Helium	-271	-261	-271	-269
2	Nitrogen	-210	-196	-203	-160
3	Ammonia	-78	-33	-60	100
4	Pentane	-130	28	-20	120

5	Acetone	-95	57	0	120
6	Methanol	-98	64	10	130
7	Flutec PP2	-50	76	10	160
8	Ethanol	-112	78	0	130
9	Heptane	-90	98	0	150
10	Water	0	100	30	200
11	Flutec PP9	-70	160	0	225
12	Mercury	-39	361	250	650
13	Caesium	29	670	450	900
14	Potassium	62	774	500	1000
15	Sodium	98	892	600	1200
16	Lithium	179	1340	1000	1800

Properties of Compatible Materials

Copper

Compatible Fluids	Yield Strength of pipe material (MPa)	Contact Angle (^{0})	Pore Radius (cm)	Permeability (x 10^{10} m2)	Porosity (%)	Thermal Conductivity of material (W/mK)
Acetone	200	14.18	0.0009	0.0174	0.52	394
Methanol	200	12	0.0009	0.0174	0.52	394
Water	200	61.5	0.0009	0.0174	0.52	394

Aluminium

Compatible Fluids	Yield Strength of pipe material (MPa)	Contact Angle (^{0})	Pore Radius (cm)	Permeability (x 10^{10} m2)	Porosity (%)	Thermal Conductivity of material (W/mK)
Ammonia	210	0.01	0.019	0.78	0.4	205
Acetone	210	9.93	0.019	0.78	0.4	205

Stainless Steel

Compatible Fluids	Yield Strength of pipe material (MPa)	Contact Angle (^{0})	Pore Radius (cm)	Permeability (x 10^{10} m2)	Porosity (%)	Thermal Conductivity of material (W/mK)
Ammonia	241	0.01	0.013	2.57	0.4	17.3
Acetone	241	10	0.013	2.57	0.4	17.3

Nickel

Compatible Fluids	Yield Strength of pipe material (MPa)	Contact Angle (^{0})	Pore Radius (cm)	Permeability (x 10^{10} m2)	Porosity (%)	Thermal Conductivity of material (W/mK)
Ammonia	105.5	0.01	0.004	0.62	0.689	88
Acetone	105.5	11.5	0.004	0.62	0.689	88
Methanol	105.5	11.5	0.004	0.62	0.689	88
Water	105.5	0.01	0.004	0.62	0.689	88
Potassium	105.5	0.01	0.004	0.62	0.689	88

Titanium

Compatible Fluids	Yield Strength of pipe material (MPa)	Contact Angle (^{0})	Pore Radius (cm)	Permeability (x 10^{10} m2)	Porosity (%)	Thermal Conductivity of material (W/mK)
Caesium	275	0.01	0.0015	0.302	0.68	21.9

Tungsten

Compatible Fluids	Yield Strength of pipe material (MPa)	Contact Angle (^{0})	Pore Radius (cm)	Permeability (x 10^{10} m2)	Porosity (%)	Thermal Conductivity of material (W/mK)
Lithium	72.4	0.01	0.017	6	0.89	173

Niobium

Compatible Fluids	Yield Strength of pipe material (MPa)	Contact Angle (^{0})	Pore Radius (cm)	Permeability (x 10^{10} m2)	Porosity (%)	Thermal Conductivity of material (W/mK)
Sodium	300	0.01	0.052	4.15	0.4	53.7
Lithium	300	0.01	0.052	4.15	0.4	53.7

9. MATLAB code

The MATLAB code for the entire run is attached for reference below :

```
prompt={'Minimum Operating Temperature(Tmin degree celsius)*','Maximum Operating Temperature(Tmax degree
celsius)*','Ambient Temperature(Tamb degree celsius)','Heat Load Generated (Q watts)*','Length of
Evaporator(centimeters)*','Lengthh of Condensor(centimeters)','Effective lenght of Heat
Pipe(centimeters)','Limiting Vapor-space Area(Sq. centimeters)','Angle of Inclination of Heat
pipe(degrees)'};
title='Heat Pipe Design';
def={'','','27','','','8','50','0.5','0'};
num=1;
h = msgbox('Fields marked with * are to be filled compulsorily');
uiwait(h);
answer=inputdlg(prompt,title,num,def);
Tmi = str2num(answer{1});
Tmin = Tmi+273;
Tma = str2num(answer{2});
Tmax = Tma+273;
Tam = str2num(answer{3});
Tamb = Tam+273;
Q = str2num(answer{4});
Leva = str2num(answer{5});
Levap = Leva/100;
Lcon = str2num(answer{6});
Lcond = Lcon/100;
Lef = str2num(answer{7});
Leff = Lef/100;
Are = str2num(answer{8});
Area1 = Are/10000;
Thet = str2num(answer{9});
Theta = Thet/pi;


load('fluids_data.mat');
load('materials_data.mat');

% Primitive Design
        FluidName = {'Helium';'Nitrogen';'Ammonia';'Pentane';'Acetone';'Methanol';'Flutec
PP21';'Ethanol';'Heptane';'Water';'Flutec PP91';'Mercury ';'Caesium';'Potassium';'Sodium';'Lithium'};
        MaterialName = {'Copper';'Aluminium';'Stainless Steel';'Nickel';'Titanium';'Tungsten';'Nb+ 1% Zr'};
%   Fluid = zeros(2,10,16);
%       Material = zeros(6,7,16);
        [~,Fluid,Material] = fluid_selection(Tmin,Tmax); %Return fluids that are compatible

    if Area1 ~= 0
                Qcrit= Q/Area1;
        else
                Area1 = 4*1.9635e-05; %Default diameter assumed to be 1 cm
                Qcrit= Q/Area1;
    end


        %Entrainment Limit
```

```
        EntAccept = zeros(1,16);
        Qent= zeros(1,16);
        for j=1:16
                Qent(1,j)=Area1*Fluid(2,2,j)*sqrt((2*pi*Fluid(2,4,j)*Fluid(2,1,j))/0.000036);
                if (Q < Qent(1,j))
                        EntAccept(1,j) = 1;
                end
    end


        %Sonic Limit
        SonAccept = zeros(1,16);
        Qson = zeros(1,16);
        for i=1:16
         if (Fluid(1,8,i) ~=0)
             rw(1,i) = 8315/Fluid(1,8,i); %Characteristic Gas Constant
         else
             rw(1,i) = 0; %Characteristic Gas Constant
         end
                Qson(1,i)= Fluid(1,4,i)*Fluid(1,2,i)*sqrt((Fluid(1,7,i)*rw(1,i)*Tmin)/(2*(Fluid(1,7,i)+1)));
                if (Qcrit < Qson(1,i))
                        SonAccept(1,i) = 1;
                end
    end


        %Wicking Limit
        MerAccept = zeros(1,16);
        Mer = zeros(1,16);
        for i=1:16
                if(Fluid(1,5,i)~=0)
                        Mer(1,i)= Fluid(1,3,i)*Fluid(1,1,i)*Fluid(1,2,i)/Fluid(1,5,i);   %Code for checking
Merit Limit later
                end
    end


        %Radial Heat Flux Limit
        Tsup = zeros(1,16);
        for i=1:16
                if(Fluid(2,4,i)~=0)
                        Tsup(1,i) = (3.06*Fluid(2,1,i)*Tmax)/(Fluid(2,4,i)*Fluid(2,2,i)*15e-6);
                end
    end


        %Best Fluid
        Normvalue = zeros(1,16);
        Tsupmax = max(Tsup);
        Mermax = max(Mer);
        for i=1:16
                        Normvalue(1,i) = 0.5*((Tsup(1,i)/Tsupmax)+(Mer(1,i)/Mermax));
        end
        [~,Best] = max(Normvalue);


        %Thickness Limit
        t = zeros(16,7);
        for i=1:16
                for j=1:7
                        if(Material(1,j,i) ~= 0)
```

```
                        t(i,j) = Fluid(1,9,i)*sqrt(Area1/pi)/Material(1,j,i);
                    end

            end
    end


        %Burnout Limit
        BurnAccept = zeros(1,16);
        Qburn = zeros(1,16);
        for i=1:16
         if (Fluid(2,4,i) ~= 0)
             Qburn(1,i)= 0.012*Fluid(2,2,i)*Fluid(2,4,i)*(((Fluid(2,3,i)-Fluid(2,4,i))/(Fluid(2,4,i)))^0.6);
         end
                if (Qcrit < Qburn(1,i))
                        BurnAccept(1,i) = 1;
                end
    end


        % Detailed Design
        syms x;
        Dw = zeros(16,7);
        for i=1:16
                for j =1:7
                        if ((Fluid(2,4,i)~=0) && (Material(2,j,i)~=0))
                                Reax = (Q/(pi*sqrt(Area1/pi)*Fluid(2,5,i)*Fluid(2,2,i)));
                                if (Reax < 1000)
                                        Pliq = (0.074*Q/(Fluid(2,2,i)*Fluid(2,4,i)*((Area1/pi)^2)))+
((8*Fluid(2,6,i)*Q*(Leff-((Lcond+Levap)/2)))/(Fluid(2,2,i)*pi*Fluid(2,4,i)*((Area1/pi)^2)));
                                else
                                        Pliq = (0.074*Q/(Fluid(2,2,i)*Fluid(2,4,i)*((Area1/pi)^2)))+
((0.0791*Fluid(2,4,i)*(Q^2)*(Leff-
((Lcond+Levap)/2)))/((Reax^0.25)*(Fluid(2,2,i)^2)*(Fluid(2,4,i)^2)*(Area1^2)*sqrt(Area1/pi)));
                                end
                                eqn = ((4*Fluid(2,5,i)*Q*Leff)/(Fluid(2,3,i)*Fluid(2,2,i)*pi*((x^2)-
(2*sqrt(Area1/pi)))*Material(4,j,i)))+(9.81*Fluid(2,4,i)*(Leff+x)*sin(pi*Theta/180))+Pliq-
(2*Fluid(2,2,i)*cos(Material(2,j,i))/Material(3,j,i))== 0;
                                solx  = solve(eqn,x);
                                if (solx(1,1)>0)
                            Dw(i,j) = solx(1,1);
                         else
                            Dw(i,j) = solx(2,1);
                         end
                        end
                end
    end


        %Power Estimation
        h = zeros(16,7);
        kw = zeros(16,7);
        Z = zeros(16,7);
        v = zeros(16,7);
        Pow = zeros(16,7);
        for i=1:16
                for j =1:7
                        if ((Fluid(2,2,i)~=0) && (Material(6,j,i)~=0))
                                Qdot = Q*Fluid(1,2,i)/Fluid(2,2,i);
                                kw(i,j) = ((1-
Material(5,j,i))*Material(6,j,i))+(Material(5,j,i)*Fluid(1,10,i));
```

```
                                Z(i,j)=(((Tmin-Tamb)/Qdot)-
((log(Dw(i,j)/(2*sqrt(Area1/pi))))/(2*pi*kw(i,j)*Lcond))-
((log((Dw(i,j)+2*t(i,j))/Dw(i,j)))/(2*pi*Material(6,j,i)*Lcond)));
                                h(i,j)=(1/(Z(i,j)*(pi/4*((Dw(i,j)+2*t(i,j))^2))));
                                Pr = 0.80377 - (0.5531*Tamb/1000) + (0.9090*(Tamb/1000)^2);
                                k = 5.9776e-04*((Tamb^1.5)/(Tamb+194.4))/4.18;
                                f = (h(i,j)*(Dw(i,j)+2*t(i,j))/k)/(Pr^0.333);
                                Re1 = (f/0.989)^(1/0.333);
                                Re2 = (f/0.911)^(1/0.385);
                                Re3 = (f/0.683)^(1/0.466);
                                Re4 = (f/0.193)^(1/0.618);
                                Re5 = (f/0.027)^(1/0.805);
                                if (Re1 >= 0.4 && Re1 <= 4)
                                        Re = Re1;
                                        break
                                elseif (Re2 >= 4 && Re2 <= 40)
                                        Re = Re2;
                                        break
                                elseif (Re3 >= 40 && Re3 <= 4000)
                                        Re = Re3;
                                        break
                                elseif (Re4 >= 4000 && Re4 <= 40000)
                                        Re = Re4;
                                        break
                                else
                                        Re = Re5;
                                end
                                mu = Pr*k/1005;
                                v(i,j) = Re*mu/((Dw(i,j)+2*t(i,j))*1.12);
                                Pow(i,j) = 0.5*1.12*(v(i,j)^2);
                        end
                end
        end

        %Output Variable Declaration and Allocation
        ind=1;
        for i=1:16
            if(Fluid(:,2,i) ~= 0)
                index(ind) = i;
                ind = ind+1;
            end
        end

        matind=1;
        for k = 1:ind-1
            matind=1;
            for j=1:7
                if (Material(:,j,index(k))~=0)
                    materialindex(k,matind)= j;
                    matind = matind+1;
                end
            end
        end

        [matxind,matyind] = size(materialindex);

        for k = 1:ind-1
            OpFluidName(k)=FluidName(index(k));
            OpQent(1,k) = Qent(1,index(k));
            OpQson(1,k) = Qson(1,index(k));
            OpMer(1,k) = Mer(1,index(k));
```

```
        OpTsup(1,k) = Tsup(1,index(k));
        OpQburn(1,k) = Qburn(1,index(k));
    end

    for k = 1:matxind
        for l =1:matyind
            if(materialindex(k,l)~=0)
                OpMaterialName(k,l) = MaterialName(materialindex(k,l));
                Opt(k,l)=t(index(k),materialindex(k,l));
                OpDw(k,l)=Dw(index(k),materialindex(k,l));
                OpPow(k,l)=Pow(index(k),materialindex(k,l));
            end
        end
    end

F = figure('position',[600,0,700,800]);
T = uicontrol(F,'Style','text','Position',[0 0 700 800]);
o = ['Qin = ',num2str(Q),' Watts      Tmin = ',num2str(Tmi),' deg celsius       Tmax = ',num2str(Tma),' deg
celsius'];
T = uicontrol(F,'Style','text','String',o,'Position',[0 0 700 800]);

for i=1:ind-1
    T = uicontrol(F,'Style','Text','String',OpFluidName(i),'Position',[200 880-180*i 150 20]);
    p = ['Qsonic = ',num2str(OpQson(1,i)),' Watts  Qentrainment = ',num2str(OpQent(1,i)),' Watts  Merit no.=
',num2str(OpMer(1,i)),'   Tsuperheat = ',num2str(OpTsup(1,i)),' kelvin   Qburnout =
',num2str(OpQburn(1,i)),' Watts'];
    T = uicontrol(F,'Style','Text','String',p,'Position',[40 850-180*i 500 30]);

    rnames = {'Tube Thickness','Wick Diameter','Fan Specific Power'};
    cnames = {OpMaterialName(1,l),OpMaterialName(2,l),OpMaterialName(3,l),OpMaterialName(4,l)};
    d = [Opt(1,l) Opt(2,l) Opt(3,l) Opt(4,l) Opt(5,l);OpDw(1,l) OpDw(2,l) OpDw(3,l) OpDw(4,l)
OpDw(5,l);OpPow(1,l) OpPow(2,l) OpPow(3,l) OpPow(4,l) OpPow(5,l)];

    w = uitable(F,'Data',d,'ColumnName',cnames,'RowName',rnames,'Position',[0 760-180*i 700 100]);
    w.Position(3) = w.Extent(3);
    w.Position(4) = w.Extent(4);

end
```

Published with MATLAB® R2014a

10. Bibliography

[1] "T.P. Cotter, Theory of heat pipes, LA-3246-MS, March 26, 1965."

[2] "J. Bohdansky, H.E.J. Schins, The temperature dependence of liquid metals, J. Chem. Phys. 49 (1968) 2982.".

[3] " J.K. Fink, L. Leibowitz, Thermodynamic and transport properties of sodium liquid and vapor, ANL/RE-95/2, Argonne National Laboratory, January 1995.".

[4] "T. Iida, R.I.L. Guthrie, The Physical Properties of Liquid Metals, Clarendon Press, Oxford, 1988.".

[5] "J.J. Jasper, The surface tension of pure liquid compounds, J. Phys. Chem. Ref. Data 1 (1972) 841.".

[6] "C.A. Busse, Pressure drop in the vapour phase of long heat pipes. Thermionic Conversion Specialists Conference, Palo Alto, CA, October 1967.".

[7] "G.M. Grover, J.E. Kemme, E.S. Keddy, Advances in heat pipetechnology, Second International Symposium on Thermionic Electrical Power Generation, Stresa, Italy, May 1968.".

[8] "D.M. Ernst, Evaluation of theoretical heat pipe performance, Thermionic Specialist Conference, Palo Alto, CA, October 1967.".

[9] "C.A. Bankston, J.H. Smith, Incompressible laminar vapour flow in cylindrical heat pipes. ASME Paper No. 7 1-WAJHT-1 5, 1971.".

[10] "J.E. Deverall, J.E. Kemme, L.W. Flarschuetz, Some limitations and startup problems of heat pipes, LA-4518, November 1970.".

[11] "H.A. Cheung, Critical review of heat pipe theory and applications, UCRL50453, July 1968.".

[12] "S. Nukiyama, Maximum and minimum values of heat transmitted from metal to boiling water under atmospheric pressure, J. Soc. Mech. Eng. Japan 37 (1934) 367.".

[13] "Y.Y. Hsu, On the size range of active nucleation cavities on a heating surface, ASME J. Heat Transfer (August 1962).".

[14] "W.M. Rosenhow, P. Griffith, Correlation of maximum heat flux data for boiling of saturated liquids. ASME _ AIChE Heat Transfer Symposium, Louisville, KY, 1955.".